

Article

Hyperspectral Image Classification Based on Semi-Supervised Rotation Forest

Xiaochen Lu * , Junping Zhang *, Tong Li and Ye Zhang

School of Electronics and Information Engineering, Harbin Institute of Technology, Harbin 150001, China; ltong@hit.edu.cn (T.L.); zhye@hit.edu.cn (Y.Z.)

* Correspondence: lxchen09@163.com (X.L.); zhangjp@hit.edu.cn (J.Z.); Tel.: +86-0451-8640-3020 (J.Z.)

Received: 20 July 2017; Accepted: 1 September 2017; Published: 6 September 2017

Abstract: Ensemble learning is widely used to combine varieties of weak learners in order to generate a relatively stronger learner by reducing either the bias or the variance of the individual learners. Rotation forest (RoF), combining feature extraction and classifier ensembles, has been successfully applied to hyperspectral (HS) image classification by promoting the diversity of base classifiers since last decade. Generally, RoF uses principal component analysis (PCA) as the rotation tool, which is commonly acknowledged as an unsupervised feature extraction method, and does not consider the discriminative information about classes. Sometimes, however, it turns out to be sub-optimal for classification tasks. Therefore, in this paper, we propose an improved RoF algorithm, in which semi-supervised local discriminant analysis is used as the feature rotation tool. The proposed algorithm, named semi-supervised rotation forest (SSRoF), aims to take advantage of both the discriminative information and local structural information provided by the limited labeled and massive unlabeled samples, thus providing better class separability for subsequent classifications. In order to promote the diversity of features, we also adjust the semi-supervised local discriminant analysis into a weighted form, which can balance the contributions of labeled and unlabeled samples. Experiments on several hyperspectral images demonstrate the effectiveness of our proposed algorithm compared with several state-of-the-art ensemble learning approaches.

Keywords: ensemble learning; hyperspectral; rotation forest; semi-supervised local discriminant analysis

1. Introduction

Hyperspectral (HS) image classification always suffers from varieties of difficulties, such as high dimensionality, limited or unbalanced training samples, spectral variability, and mixing pixels. It is well known that increasing data dimensionality and high redundancy between features might cause problems during data analysis, for example, in the context of supervised classification. A considerable amount of literature has been published with regard to overcoming these challenges, and performing hyperspectral image classification effectively [1]. Machine learning techniques such as artificial neural networks (ANNs) [2], support vector machine (SVM) [3], multinomial logistic regression [4], active learning, semi-supervised learning [5], and other methods like hyperspectral unmixing [6], object-oriented classification [7], and the multiple classifier system [8] have been popularly investigated recently as well.

Multiple classifier system (MCS), which is also sometimes named as classifier ensemble or ensemble learning (EL) in the machine learning field, is a popular strategy for improving the classification performance of hyperspectral images by combining the predictions of multiple classifiers, thereby reducing the dependence on the performance of a single classifier [8–11]. The concept of MCS, on the other hand, does not refer to a specific algorithm but to the idea of combining outputs

from more than one classifier to enhance classification accuracy [12]. These outputs may result from either the same classifier of different variants or different classifiers of the same/different training samples. Previous studies have demonstrated both theoretically and experimentally that one of the main reasons for the success of ensembles is the diversity among the individual learners (namely the base classifiers) [13], because combining similar classification results would not further improve the accuracy.

MCSs have been widely applied to HS remote sensing image classification. Two approaches for constructing classifier ensembles are perceived as “classic”, bagging and boosting [14,15], and afterwards numerous algorithms were successively derived from them. Bagging creates many classifiers with each base learner trained by a new bootstrapped training data set [16]. Boosting processes the data with iterative retraining, and concentrates on the difficult samples, with the goal of correctly classifying these samples in the next iteration [17,18]. Ho [19] proposed random subspace ensembles, which used random subsets of features instead of the entire feature set for each individual classifier. The rationale of the random subspace is to break down a complex high dimensional problem into several lower dimensional problems, thereby alleviating the curse of dimensionality. By integrating bagging and random subspace approaches, Breiman [20] proposed the well-known random forest (RF) algorithm [21,22]. The characteristics of RF, including reasonable computational cost, inherent support of parallelism, highly accurate predictions, and ability to handle a very large number of input variables without overfitting, make it a popular and promising classification algorithm for remote sensing data [23–25]. Generally, decision tree (DT) is used as the base classifier in ensemble learning because of its high computation efficiency, easy implementation, and sensitivity to slight changes in data. Recently, some researchers incorporated several prevalent machine learning algorithms into ensemble learning. Gurram and Kwon [26] proposed a sparse kernel-based support vector machine (SVM) ensemble algorithm that yields better performance compared with the SVM trained by cross-validation. Samat et al. [27] proposed Bagging-based and Adaboost-based extreme learning machines to overcome the drawbacks of input parameter randomness of traditional extreme learning machines. For a more detailed description about EL, refer to [28,29].

In a paper by Rodriguez and Kuncheva [30], the authors proposed a new ensemble classifier called rotation forest (RoF). By applying feature extraction (i.e., principal component analysis, PCA) to the random feature subspace, RoF greatly promotes the diversity and accuracy of the classifiers. Thereafter, several improved algorithms were proposed based on the idea of RoF, for example, Anticipative Hybrid Extreme Rotation Forest [31], rotation random forest with kernel PCA (RoRF-KPCA) [32]. Chen et al. [33] proposed to combine rotation forest with multi-scale segmentation for hyperspectral data classification, which incorporated spatial information to generate the classification maps with homogeneous regions.

A massive number of research studies show that RoF surpasses conventional RF due to the high diversity in training sample and features. Nevertheless, it is well documented in the literatures that PCA is not particularly suitable for feature extraction (FE) in classification because it does not include discriminative information in calculating the optimal rotation of the axes [30,34,35]. Although the authors explain that PCA is also valuable as a diversifying heuristic, it is expected to achieve better classification results if we try to find good class discriminative directions. Therefore, in this paper, we present an improved ensemble learning method, which uses the semi-supervised feature extraction technique instead of PCA during the “rotation” process of classical RoF approach. The proposed algorithm, named semi-supervised rotation forest (SSRoF), applies the semi-supervised local discriminant analysis (SLDA) FE method, which was proposed in our previous work [36], to fully take advantage of both the class separability and local neighbor information, with the aim of finding better rotation directions. In addition, to further enhance the diversity of features, we propose to use a weighted form of SLDA, which can balance the values of labeled samples and unlabeled samples. The main contributions of this paper are as follows: (1) an exploration of the benefit of the unlabeled samples in conventional ensemble learning methods; (2) an adjustment of the previous

SLDA technique to a weighted generalized eigenvalue problem; (3) the construction of an ensemble of classifiers, in which the weights can be randomly selected, thereby reducing the human effort for determining the optimal parameters.

The remainder of this paper is organized as follows. Section 2 describes the study data sets, and elaborates the proposed semi-supervised rotation forest algorithm. For better understanding, the SLDA feature extraction method is also briefly introduced. Section 3 reports the experiments and results. Finally, the conclusions are drawn in Section 4.

2. Materials and Methodology

In this section, we first introduce the experimental data sets, then we elaborate the proposed ensemble learning algorithm.

2.1. Study Data Sets

The experimental data sets include four HS images acquired by different sensors and resolutions. Each HS image is attached with a co-registered ground truth image.

- (1) The first data set is the well-known scene taken in 1992 by the Airborne Visible Infrared Imaging Spectrometer (AVIRIS) sensor over the Indian Pines region in Northwestern Indiana. It has 144×144 pixels and 200 spectral bands with a pixel resolution of 20 m. Nine classes including different categories of crops have been labeled in the ground truth image.
- (2) The second data set was collected over the University of Pavia, Italy, by the Reflective Optics System Imaging Spectrometer (ROSIS) system. It consists of 103 spectral bands after removing the noisy bands, and 610×340 pixels for each band with a pixel resolution of 1.3 m. The ground truth image contains nine classes [37,38].
- (3) The third data set is a low-altitude AVIRIS HS image of a portion of the North Island of the U.S. Naval Air Station in San Diego, CA, USA. This HS image consists of 126 bands of size 400×400 pixels with a spatial resolution of 3.5 m per pixel after removing the noisy bands. The ground truth image has eight classes inside [39].
- (4) The last data set is provided by the 2013 Institute of Electrical and Electronics Engineers (IEEE) Geoscience and Remote Sensing Society (GRSS) Data Fusion Contest (DFC). It was acquired by the compact airborne spectrographic imager sensor (CASI) over the University of Houston campus and neighboring urban area, and consists of 144 bands with a spatial resolution of 2.5 m. A subset of size 640×320 is used, which contains 12 classes in the corresponding ground truth image. Figure 1 shows the experimental data sets.

2.2. Weighted Semi-Supervised Local Discriminant Analysis

Semi-supervised local discriminant analysis is a semi-supervised feature extraction method that has been applied in hyperspectral image classification. It combines the supervised FE method-local Fisher discriminant analysis and unsupervised FE method-neighborhood preserving embedding, and thus attempts to discover the local discriminative information of the data while preserving the local neighbor information [36]. Compared with other typical semi-supervised FE methods, SLDA focuses more on the exploration of local information, and gives a more accurate description of the distribution of samples. For better illustration, we first briefly review the feature extraction methods.

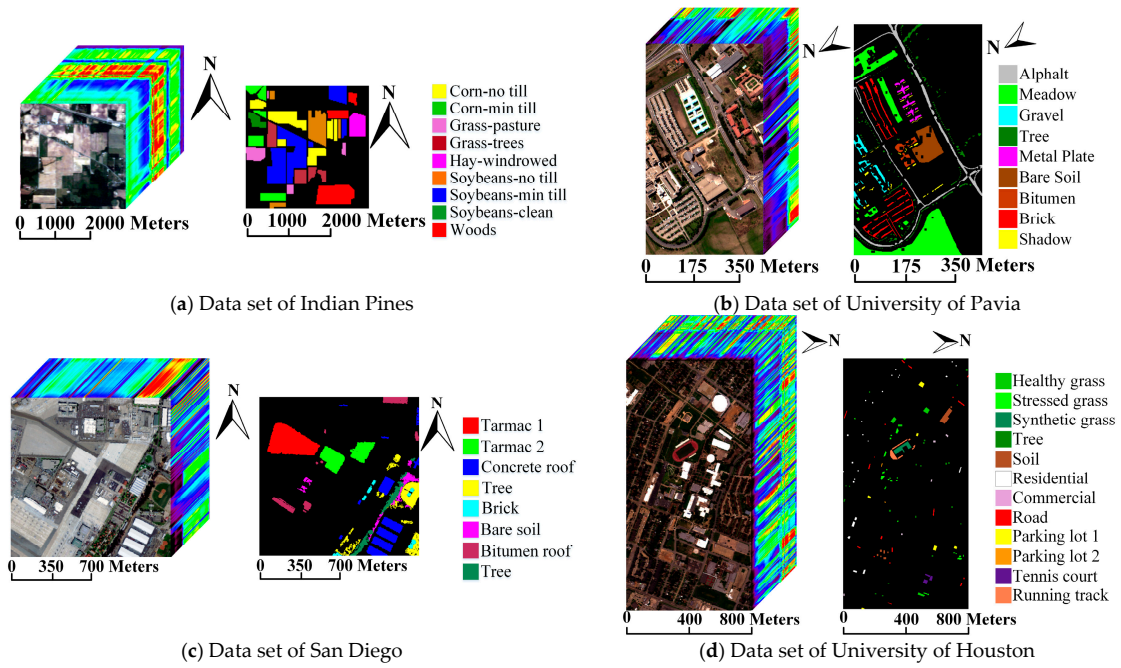


Figure 1. Experimental hyperspectral and corresponding ground truth images.

Let $x_i \in \mathbb{R}^d$ be a d -dimensional sample vector, and $X = \{x_i\}_{i=1}^n$ be the matrix of n samples. $Z = T^T X$, ($Z \in \mathbb{R}^{r \times n}$) is the low-dimensional representation of the sample matrix, where $T \in \mathbb{R}^{d \times r}$ is the transformation matrix, T denotes the transpose.

Many dimensionality reduction techniques developed so far involve an optimization problem of the following form [40]:

$$T = \operatorname{argmax}_T \left[\frac{|T^T S^b T|}{|T^T S^w T|} \right] \quad (1)$$

Generally speaking, S^b (and S^w) corresponds to the quantity that we want to increase (and decrease), for example, between-class scatter (and within-class scatter). Equation (1) is equal to the solution of the following generalized eigenvalue problem:

$$S^b \varphi = \lambda S^w \varphi \quad (2)$$

where $\{\varphi_k\}_{k=1}^d$ is the generalized eigenvectors associated with the generalized eigenvalues $\{\lambda_k\}_{k=1}^d$, ($\lambda_1 > \lambda_2 > \dots > \lambda_d$). $T = \{\varphi_k\}_{k=1}^r$ is composed of the first r eigenvectors corresponding to the largest eigenvalues $\{\lambda_k\}_{k=1}^r$. Particularly, when S^b is the total scatter matrix of all samples, and $S^w = I_{d \times d}$, where I denotes the identity matrix. Equation (1) turns into the PCA method.

2.2.1. Local Fisher Discriminant Analysis (LFDA)

Suppose $y_i = c$, $c \in \{1, 2, \dots, C\}$ is the associated class labels of the sample vector x_i . C is the number of classes. n_c is the number of samples in class c , then $\sum_{c=1}^C n_c = n$. Let S^b and S^w be the local between-class and within-class scatter matrices, respectively, defined by [41],

$$\begin{aligned} S^b &= \frac{1}{2} \sum_{i=1}^n \sum_{j=1}^n W_{i,j}^b (x_i - x_j) (x_i - x_j)^T \\ S^w &= \frac{1}{2} \sum_{i=1}^n \sum_{j=1}^n W_{i,j}^w (x_i - x_j) (x_i - x_j)^T \end{aligned} \quad (3)$$

then Equation (2) turns into a local Fisher discriminant analysis problem, where \mathbf{W}^b and \mathbf{W}^w are $n \times n$ matrices,

$$\mathbf{W}_{i,j}^b = \begin{cases} A_{i,j}(1/n - 1/n_c), & \text{if } y_i = y_j = c \\ 1/n, & \text{if } y_i \neq y_j \end{cases} \quad (4)$$

$$\mathbf{W}_{i,j}^w = \begin{cases} A_{i,j}/n_c, & \text{if } y_i = y_j = c \\ 0, & \text{if } y_i \neq y_j \end{cases}$$

$A_{i,j}$ is the affinity value between x_i and x_j . $A_{i,j}$ is large if the two samples are close, and vice versa. The definition of $A_{i,j}$ can be found in [42]. Note that we do not weight the values for the sample pairs in different classes. If $\forall i, j$, $A_{i,j} = 1$, then LFDA degenerates into the classical Fisher discriminant analysis (FDA or linear discriminant analysis, LDA) [43]. Thus, LFDA can be regarded as a localized variant of FDA, which overcomes the weakness of LDA against within-class multimodality or outliers.

2.2.2. Neighborhood Preserving Embedding (NPE)

NPE is an unsupervised feature extraction method that seeks a projection that preserves neighboring data structure in the low-dimensional feature space [44]. It can characterize the local structural information of massive unlabeled samples. The first step of NPE is also to construct an adjacency graph, and then compute the weight matrix \mathbf{Q} by solving the following objective function,

$$\min \sum_i \|x_i - \sum_j \mathbf{Q}_{ij}x_j\|^2$$

$$s.t. \sum_j \mathbf{Q}_{ij} = 1 \quad (5)$$

In other words, for each sample, we use its K-nearest neighbors (KNN) to reconstruct it. Thus, the goal of NPE is to preserve this neighbor relationship in the projected low-dimensional space,

$$\min \sum_i \|z_i - \sum_j \mathbf{Q}_{ij}z_j\|^2$$

$$s.t. \sum_j \mathbf{Q}_{ij} = 1 \quad (6)$$

where $z_i = \mathbf{T}^T x_i$. Then we have

$$\min_{\text{trace}} [\mathbf{Z}(\mathbf{I} - \mathbf{Q})^T (\mathbf{I} - \mathbf{Q}) \mathbf{Z}^T] \quad (7)$$

By imposing the following constraint,

$$\sum_i z_i z_i^T = \mathbf{I} \implies \mathbf{Z}\mathbf{Z}^T = \mathbf{I}. \quad (8)$$

the transformation matrix can be optimized by solving the following generalized eigenvalue problem,

$$\mathbf{X}\mathbf{X}^T \varphi = \lambda \mathbf{X}\mathbf{M}\mathbf{X}^T \varphi \quad (9)$$

where φ denotes generalized eigenvectors, and $\mathbf{M} = (\mathbf{I} - \mathbf{Q})^T (\mathbf{I} - \mathbf{Q})$.

2.2.3. Weighted SLDA

It has been demonstrated that the performance of LFDA (and all other supervised dimensionality reduction methods) tends to degrade if only a small number of labeled samples are available [40], while PCA or NPE (and other unsupervised feature extraction (FE) methods) will generally lose the discriminative information of labeled information. Thus, combining supervised and unsupervised FE methods [45] is believed to compensate for each other's weaknesses. In this paper, we consider the combination of the aforementioned LFDA and NPE methods. As mentioned above, feature extraction

techniques can be transformed into eigenvalue problems, thus, a possible way to combine LFDA and NPE is to merge the above generalized eigenvalue problems as follows [40],

$$\begin{aligned}
 \beta S^b \varphi &= \lambda \beta S^w \varphi \\
 (1 - \beta) \mathbf{X} \mathbf{X}^T \varphi &= \lambda (1 - \beta) \mathbf{X} \mathbf{M} \mathbf{X}^T \varphi \\
 &\Downarrow \\
 [\beta S^b + (1 - \beta) \mathbf{X} \mathbf{X}^T] \varphi & \\
 &= \lambda [\beta S^w + (1 - \beta) \mathbf{X} \mathbf{M} \mathbf{X}^T] \varphi
 \end{aligned}
 \tag{10}$$

where $\beta \in [0, 1]$ is a trade-off parameter. Calculating the S^b and S^w of LFDA is time-consuming; an efficient implementation can be used according to [41]. Let S^m denote the local mixture scatter matrix,

$$S^m = S^b + S^w = \frac{1}{2} \sum_{i=1}^n \sum_{j=1}^n W_{i,j}^m (x_i - x_j)(x_i - x_j)^T
 \tag{11}$$

where

$$W^m = W^b + W^w = \begin{cases} A_{i,j}/n, & \text{if } y_i = y_j \\ 1/n, & \text{if } y_i \neq y_j \end{cases}
 \tag{12}$$

Since Equation (3) can be expressed as

$$\begin{aligned}
 S^w &= \sum_{i=1}^n \sum_{j=1}^n W_{i,j}^w x_i x_i^T - \sum_{i=1}^n \sum_{j=1}^n W_{i,j}^w x_i x_j^T \\
 &= \mathbf{X}(\mathbf{D}^w - \mathbf{W}^w) \mathbf{X}^T
 \end{aligned}
 \tag{13}$$

where \mathbf{D}^w is the n -dimensional diagonal matrix with $D_{i,i}^w = \sum_{j=1}^n W_{i,j}^w$. Similarly, S^m can be expressed as

$$S^m = \mathbf{X}(\mathbf{D}^m - \mathbf{W}^m) \mathbf{X}^T
 \tag{14}$$

where \mathbf{D}^m is the n -dimensional diagonal matrix with $D_{i,i}^m = \sum_{j=1}^n W_{i,j}^m$. Therefore, the generalized eigenvalue problem of LFDA, namely Equation (2), can be rewritten as

$$\mathbf{X} \mathbf{L}^b \mathbf{X}^T \varphi = \lambda \mathbf{X} \mathbf{L}^w \mathbf{X}^T \varphi
 \tag{15}$$

where $\mathbf{L}^w = \mathbf{D}^w - \mathbf{W}^w$, $\mathbf{L}^b = (\mathbf{D}^m - \mathbf{W}^m) - (\mathbf{D}^w - \mathbf{W}^w)$, from which we can see that the eigenvalue problem of LFDA has a similar form with NPE, i.e., Equation (9).

Suppose the training sample vectors are arranged by $\mathbf{X} = [\mathbf{X}^L, \mathbf{X}^U]$, where $\mathbf{X}^L = \{x_i^L\}_{i=1}^{n_l}$ denotes the labeled samples, and $\mathbf{X}^U = \{x_i^U\}_{i=1}^{n_u}$ denotes the unlabeled samples, where $n = n_l + n_u$ is the total number of available samples. We can define the following matrices

$$\begin{aligned}
 \mathbf{P}_1 &= \begin{bmatrix} \mathbf{L}^b & \mathbf{0}_{n_l \times n_u} \\ \mathbf{0}_{n_u \times n_l} & \mathbf{0}_{n_u \times n_l} \end{bmatrix}, \mathbf{P}_2 = \begin{bmatrix} \mathbf{L}^w & \mathbf{0}_{n_l \times n_u} \\ \mathbf{0}_{n_u \times n_l} & \mathbf{0}_{n_u \times n_u} \end{bmatrix} \\
 \mathbf{P}_3 &= \begin{bmatrix} \mathbf{0}_{n_l \times n_l} & \mathbf{0}_{n_l \times n_u} \\ \mathbf{0}_{n_u \times n_l} & \mathbf{I}_{n_u \times n_u} \end{bmatrix}, \mathbf{P}_4 = \begin{bmatrix} \mathbf{0}_{n_l \times n_l} & \mathbf{0}_{n_l \times n_u} \\ \mathbf{0}_{n_u \times n_l} & \mathbf{M} \end{bmatrix}
 \end{aligned}
 \tag{16}$$

Therefore, the weighted SLDA is equal to the solution of the following generalized eigenvalue problem

$$\begin{aligned}
\beta \mathbf{X} \mathbf{P}_1 \mathbf{X}^T \varphi &= \lambda \beta \mathbf{X} \mathbf{P}_2 \mathbf{X}^T \varphi \\
(1 - \beta) \mathbf{X} \mathbf{P}_3 \mathbf{X}^T \varphi &= \lambda (1 - \beta) \mathbf{X} \mathbf{P}_4 \mathbf{X}^T \varphi \\
&\Downarrow \\
\mathbf{S}^{rb} &= \mathbf{X} [\beta \mathbf{P}_1 + (1 - \beta) \mathbf{P}_3] \mathbf{X}^T \\
\mathbf{S}^{rw} &= \mathbf{X} [\beta \mathbf{P}_2 + (1 - \beta) \mathbf{P}_4] \mathbf{X}^T \\
&\Downarrow \\
\mathbf{S}^{rb} \varphi &= \lambda \mathbf{S}^{rw} \varphi
\end{aligned} \tag{17}$$

and β is the trade-off parameter. In general, $0 < \beta < 1$ inherits the characteristics of both LFDA and NPE, and thus makes full use of both the class discriminative and local neighbor spatial information. In practice, searching for the optimal β is time-consuming and sometimes impractical if there are insufficient labeled samples available for validation. Several research studies suggest that ensemble learning methods can be employed to avoid the huge effort of searching for the optimal parameters [46,47]. On the other hand, different parameters also lead to diversity among features or classifiers, which benefits the generalization performance of the ensembles. Hence, we present an EL method based on the idea of RoF and the weighted SLDA algorithm.

2.3. Proposed Semi-Supervised Rotation Forest

Rotation forest was developed from conventional random forest to building independent decision trees on different sets of features. It consists of splitting the feature set into several random disjoint subsets, running PCA separately on each subset, and reassembling the extracted features [30,48]. By applying different splits of the features, diverse classifiers are obtained. The main steps of RoF are briefly presented as follows:

1. The original feature set is divided randomly into K disjoint subsets with each subset containing M features;
2. Use the bootstrap approach to select a subset of the training samples for each feature subset (typically 75% of the total training samples);
3. Run PCA on each feature subset and store the transformation coefficients;
4. Reorder the coefficients to match the original features, rotate the samples using the obtained coefficients (i.e., feature extraction);
5. Perform DT on the rotated training and testing samples;
6. The process is repeated L times to obtain multiple classifiers, followed by a majority voting rule to integrate the classification results.

By substituting SLDA for the PCA method, we propose the following SSRoF ensemble algorithm. Apart from the different FE methods between Algorithm 1 and RoF, we use the different weights (β) to balance the discriminative information and structure information, thereby enhancing the diversity of features. Although the computation of the eigenvector matrix is repeated ten times (corresponding to different β) for each feature subset, it can be noticed that since the within-class and between-class scatter matrices are invariant for different weights, the computation cost is greatly reduced. Of course, the discrete values of β can be set by different steps; we recommend the values above by considering both the diversity and computation time.

Algorithm 1: Procedures of SSRoF

Input: Training samples $X^L = \{x_i^L\}_{i=1}^{n_l}$, testing samples $X^T = \{x_i^T\}_{i=1}^{n_t}$, unlabeled samples $X^U = \{x_i^U\}_{i=1}^{n_u}$, ensemble classifiers L , number of feature subsets K , ensemble $\mathcal{L} = \emptyset$

Output: Class labels of X^T

For $i = 1 : L$

1. Randomly split the features into K subsets;

For $j = 1 : K$

2. Randomly select a subset of samples from X^L and X^U , respectively, (typically 75% of samples) using bootstrap approach;
3. Perform the weighted SLDA algorithm by the subset of X^L and X^U to obtain the pairs of between-class and within-class scatter matrices in Equation (17);

For $\beta = 0.1 : 0.1 : 1$

4. Obtain the eigenvector matrix $T_{j,\beta}$ by solving Equation (17);

End for

End for

For $\beta = 0.1 : 0.1 : 1$

5. Construct the transformation matrix $T_\beta = [T_{1,\beta}, T_{2,\beta}, \dots, T_{K,\beta}]$ by merging the eigenvector matrices, and rearrange the columns of T_β to match the order of original features;
6. Build DT sub-classifier using $T_\beta^T X^L$;
7. Perform classification for $T_\beta^T X^T$ by using the sub-classifier;

End for

End for

8. Use a majority voting rule for the $L \times 10$ sub-classifiers to compute the confidence of X^T and assign a class label for each testing sample;

3. Experimental Results and Discussion

In this section, we report the experiments on the four groups of hyperspectral images. First, the presented method is compared with several other EL algorithms to show the advantages. Then, we also introduce the performance evaluation of our method under different parameters.

3.1. Experimental Setup

In order to demonstrate the advantages of the proposed algorithm, we conducted the experiments under different numbers of training samples, and compared with several state-of-the-art ensemble learning methods, namely random forest (RF), semi-supervised feature extraction combined RF ensemble method (SSFE-RF) [22], rotation forest (RoF) [30], and rotation random forest-KPCA (RoRF-KPCA) [32]. For better comparison, the SLDA method was also used as a preprocessing step that combined with the original RoF method (we refer to it as SLDA-RoF). Finally, the LFDA and NPE methods were also used as rotation means like RoF method.

The numbers of trees were all set to $L = 10$, and the classification and regression tree (CART) was adopted as the base classifier. The numbers of features in each subset were all set to $M = 10$ for SSFE-RF, RoF, RoF-LFDA, RoF-NPE, and SSRoF. For RoRF-KPCA, Xia et al. [32] suggest that a small number of features per subset will increase the classification performance, as such, we set $M = 5$. For RF, the number of features considered at each node was set as the square root of the used feature number. The numbers of extracted features were set equal to M for RoF, RoRF-KPCA, RoF-LFDA, RoF-NPE, and SSRoF. For SLDA, the number of extracted features was set to half of the original features, and other parameters were set to the same as RoF. For RoRF-KPCA, it is quite difficult to select the optimal kernel parameters. Xia et al. [32] declares that parameter tuning is needed, but different kernel functions (linear, radial basis function, and Polynomial) provide very similar results, making this choice not critical in this context. Considering the performance enhancement and the computation cost, in our experiments, we use the polynomial kernels with the degree equals to two.

The performance is evaluated by the overall accuracy (OA), and Kappa coefficient. In all cases, we conduct ten independent Monte Carlo runs with respect to the labeled training set from the ground truth images. And the results are the average values of the 10 runs. The numbers of available samples are listed in Table 1.

Table 1. Number of available samples in each data set.

| Indian Pines | | University of Pavia | | San Diego | | University of Houston | |
|-------------------|---------|---------------------|---------|---------------|---------|-----------------------|---------|
| Class | Samples | Class | Samples | Class | Samples | Class | Samples |
| corn-no till | 1434 | asphalt | 6304 | tarmac1 | 7044 | healthy grass | 449 |
| corn-min till | 834 | meadow | 18146 | tarmac2 | 4721 | stressed grass | 454 |
| grass-pasture | 234 | gravel | 1815 | concrete roof | 5771 | synthetic grass | 505 |
| grass-trees | 497 | tree | 2912 | tree | 4851 | tree | 293 |
| hay-windrowed | 747 | metal plate | 1113 | brick | 873 | soil | 688 |
| soybeans-no till | 489 | bare soil | 4572 | bare soil | 1748 | residential | 26 |
| soybeans-min till | 968 | bitumen | 981 | bitumen roof | 2454 | commercial | 463 |
| soybeans-clean | 2468 | brick | 3364 | tree | 2135 | road | 112 |
| woods | 1294 | shadow | 795 | | | parking lot 1 | 427 |
| | | | | | | parking lot 2 | 247 |
| | | | | | | tennis court | 473 |
| | | | | | | running track | 367 |

3.2. Performance Evaluation

The comparison of different EL algorithms is presented here. We randomly selected 1%, 2%, and 5% samples of each class as training samples for the first three data sets, and 5%, 10%, and 20% for the last data set. The remaining samples were used for testing purposes. Table 2 lists the classification results of the four algorithms under different numbers of samples. The upper line in each cell denotes the overall accuracies, and the lower line is the Kappa values. For clarity, the best results are shown in different colors.

From the table, it can be seen obviously that all the other methods yielded much higher accuracies than the conventional RF method. SSFE-RF achieved higher accuracies than RF due to the increment in the number of classifiers and the semi-supervised feature extraction method. Particularly, it had splendid performance on the San Diego data set. Moreover, except for the SLDA-RoF, all of the other RoF-based approaches also surpassed the RF-based methods in most cases, which demonstrates the promotion of diversity owing to the random feature extraction. RoRF-KPCA yielded similar results with RoF, although it considers the nonlinear characteristics of hyperspectral data, and would have constructed reliable rotation matrices to generate high precision classification results. A probable reason may be the selection of sub-optimal parameters for kernel functions. However, as we have mentioned, searching for the optimal parameters remains problematic, and RoRF-KPCA is not sensitive to the changes of the kernel function. A smaller value of M may also affect the classification accuracy, although a smaller M means a larger K , which leads to a higher computational complexity due to the construction of the kernel matrix. Regardless of the computation time, it can be expected that RoRF-KPCA can surpass RoF to some extent. It can also be seen that RoF-LFDA and RoF-NPE also produced similar results as RoF. RoF-LFDA sometimes performed better than RoF and RoF-NPE when more samples were available, since it only uses the discriminative information of the labeled samples. In fact, no matter which simple rotation method was used in RoF, it seems that the results were very close to each other on the whole. However, the SLDA combined RoF method has relatively lower accuracies compared with other RoF-based method, although it has been demonstrated to perform well for other conventional classifiers [36] (e.g., MLC, SVM). Thus, it seems to be not suitable for rotation forest algorithms.

By contrast, the proposed SSRoF outperformed the others clearly in most cases from both OA and Kappa values, especially on the Indian and Pavia data sets (4.35% and 1.45% higher than RoF for the Indian and Pavia data sets on average, respectively). Although the conventional RF and RoF-based algorithms performed well on the last data set, the proposed algorithm still showed slight superiority.

The main reason why the proposed SSRoF method surpasses RoF-LFDA and RoF-NPE is that SSRoF uses a weighted form to better explore the discriminative information and structure information of the available samples, thus greatly promoting the diversity of features.

Table 2. The overall accuracies (%) and Kappa coefficients of different algorithms.

| | | RF | SSFE-RF | RoF | RoRF-KPCA | SLDA-RoF | RoF-LFDA | RoF-NPE | SSRoF |
|-----------|-----|--------|---------|--------|-----------|----------|----------|---------|--------|
| Indian | 1% | 58.35 | 66.87 | 71.48 | 70.54 | 63.88 | 66.17 | 69.39 | 74.38 |
| | | 0.5018 | 0.5995 | 0.6587 | 0.6491 | 0.5660 | 0.5943 | 0.6337 | 0.6918 |
| | 2% | 64.55 | 74.89 | 75.80 | 77.11 | 70.22 | 76.72 | 76.45 | 80.83 |
| | | 0.5746 | 0.6971 | 0.7117 | 0.7272 | 0.6437 | 0.7214 | 0.7179 | 0.7710 |
| | 5% | 70.79 | 81.04 | 82.97 | 82.96 | 77.58 | 83.01 | 82.66 | 86.84 |
| | | 0.6502 | 0.7728 | 0.7971 | 0.7971 | 0.7330 | 0.7978 | 0.7936 | 0.8429 |
| Pavia | 1% | 79.65 | 84.93 | 87.13 | 87.02 | 81.20 | 87.09 | 86.67 | 88.98 |
| | | 0.7143 | 0.7879 | 0.8223 | 0.8205 | 0.7373 | 0.8214 | 0.8152 | 0.8484 |
| | 2% | 82.38 | 87.27 | 89.54 | 89.39 | 84.34 | 90.15 | 89.61 | 91.60 |
| | | 0.7538 | 0.8220 | 0.8559 | 0.8537 | 0.7840 | 0.8645 | 0.8571 | 0.8846 |
| | 5% | 85.82 | 90.26 | 92.28 | 92.10 | 86.82 | 92.52 | 91.77 | 93.67 |
| | | 0.8029 | 0.8648 | 0.8943 | 0.8919 | 0.8186 | 0.8978 | 0.8871 | 0.9137 |
| San Diego | 1% | 86.08 | 96.07 | 95.28 | 94.19 | 93.25 | 95.20 | 95.55 | 95.99 |
| | | 0.8333 | 0.9529 | 0.9435 | 0.9305 | 0.9192 | 0.9426 | 0.9467 | 0.9520 |
| | 2% | 90.10 | 96.78 | 96.40 | 95.88 | 94.86 | 96.50 | 96.56 | 97.02 |
| | | 0.8814 | 0.9615 | 0.9569 | 0.9507 | 0.9385 | 0.9582 | 0.9589 | 0.9644 |
| | 5% | 93.10 | 97.69 | 97.64 | 97.09 | 96.40 | 97.62 | 97.61 | 98.02 |
| | | 0.9175 | 0.9724 | 0.9717 | 0.9652 | 0.9569 | 0.9716 | 0.9715 | 0.9764 |
| Houston | 5% | 91.32 | 95.97 | 96.06 | 96.08 | 93.73 | 96.06 | 96.33 | 97.43 |
| | | 0.9034 | 0.9551 | 0.9561 | 0.9564 | 0.9302 | 0.9561 | 0.9591 | 0.9714 |
| | 10% | 94.40 | 96.59 | 97.08 | 97.60 | 94.98 | 96.96 | 97.33 | 98.09 |
| | | 0.9376 | 0.9620 | 0.9676 | 0.9733 | 0.9441 | 0.9662 | 0.9703 | 0.9787 |
| | 20% | 96.31 | 98.03 | 98.18 | 98.42 | 96.54 | 98.22 | 97.77 | 98.60 |
| | | 0.9590 | 0.9780 | 0.9798 | 0.9824 | 0.9615 | 0.9802 | 0.9752 | 0.9845 |

RF: random forest; SSFE-RF: semi-supervised feature extraction combined random forest; RoF: rotation forest; RoRF-KPCA: rotation random forest with kernel principal component analysis; SLDA-RoF: RoF with semi-supervised local discriminant analysis pre-processing; RoF with local Fisher discriminant analysis; RoF-NPE: RoF with neighborhood preserving embedding; SSRoF: semi-supervised rotation forest.

Particularly, aside from the number of ensembles L and the number of features per subset (M), the proposed approach needs fewer additional parameters, which makes the approach much easier to implement.

3.3. Impact of Parameters

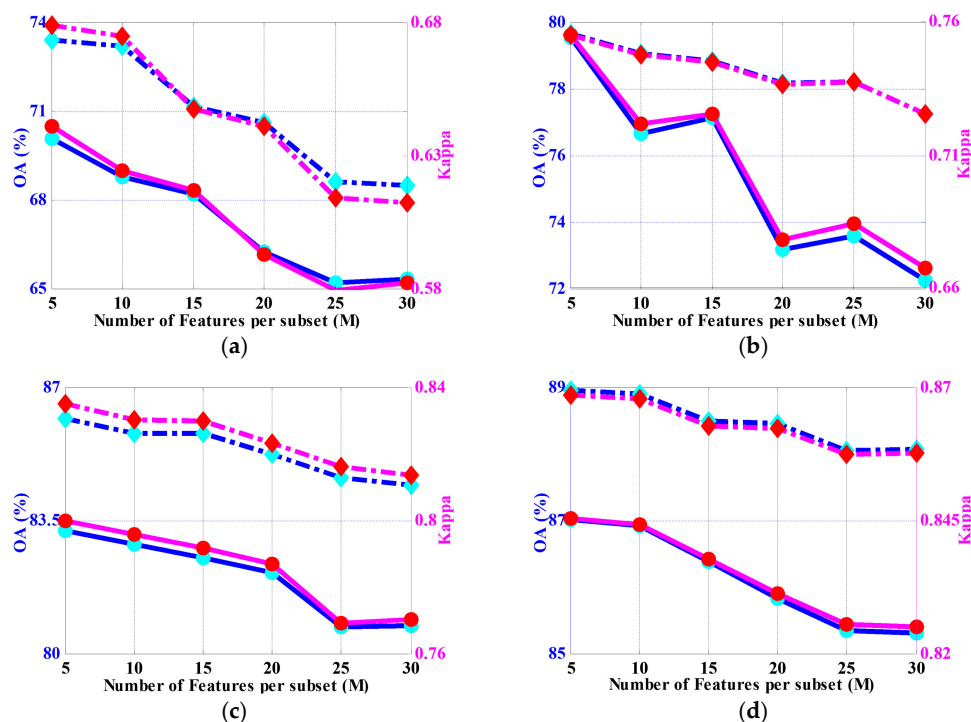
In this sub-section, we will discuss the impact of two basic parameters, i.e., the number of ensembles (L), and the number of features in each subset (M). For brevity, we simply show the results performed on the data sets of Indian Pines and University of Pavia by setting different number of trees, i.e., $L = 2, 5, 10, 20$, and 30 . Likewise, the experiments are conducted under different numbers of training samples. The results are shown in Table 3. In order to give an intuitive evaluation, OAs and Kappa values are shown in different colors.

From Table 3 we can see that, obviously, with the increment of ensemble number, the overall accuracy and Kappa coefficient grow continuously, for instance, from nearly 67% to 75% under 1% samples for the Indian Pines data set, which demonstrates the benefit of EL. An interesting factor is that when the number of trees increases to 10, the classification accuracy grows slower and tends to reach convergence. This makes our approach more promising, since we can use less ensembles to achieve a relatively stable result, thereby reducing the computational burden.

Table 3. The classification results of SSRoF under different number of ensembles (L). OA: overall accuracy.

| | | $L = 2$ | | $L = 5$ | | $L = 10$ | | $L = 20$ | | $L = 30$ | |
|--------|-----|---------|--------|---------|--------|----------|--------|----------|--------|----------|--------|
| | | OA (%) | Kappa | OA (%) | Kappa | OA (%) | Kappa | OA (%) | Kappa | OA (%) | Kappa |
| Indian | 1% | 71.01 | 0.6516 | 74.16 | 0.6887 | 74.69 | 0.6955 | 74.65 | 0.6944 | 74.96 | 0.6978 |
| | 2% | 77.91 | 0.7359 | 79.56 | 0.7545 | 80.03 | 0.7600 | 80.54 | 0.7660 | 80.95 | 0.7710 |
| | 5% | 83.55 | 0.8039 | 85.63 | 0.8285 | 86.62 | 0.8403 | 86.87 | 0.8432 | 86.97 | 0.8443 |
| | 10% | 86.51 | 0.8392 | 88.44 | 0.8622 | 88.87 | 0.8672 | 89.24 | 0.8716 | 89.26 | 0.8718 |
| | 20% | 88.91 | 0.8682 | 90.71 | 0.8894 | 91.25 | 0.8958 | 91.67 | 0.9008 | 91.74 | 0.9016 |
| Pavia | 1% | 87.71 | 0.8308 | 88.79 | 0.8456 | 89.13 | 0.8504 | 89.38 | 0.8538 | 89.45 | 0.8548 |
| | 2% | 89.74 | 0.8592 | 91.20 | 0.8794 | 91.35 | 0.8814 | 91.65 | 0.8856 | 91.75 | 0.8869 |
| | 5% | 92.13 | 0.8924 | 93.36 | 0.9094 | 93.70 | 0.9141 | 93.78 | 0.9151 | 93.86 | 0.9163 |
| | 10% | 93.07 | 0.9053 | 94.10 | 0.9195 | 94.46 | 0.9245 | 94.59 | 0.9263 | 94.59 | 0.9262 |
| | 20% | 94.48 | 0.9250 | 95.15 | 0.9341 | 95.31 | 0.9363 | 95.45 | 0.9382 | 95.46 | 0.9383 |

To investigate the impact of the number of features in each subset, we also performed tests on the Indian Pines data set regarding different feature divisions. For better comparison, the same process was also applied on RoF algorithm, and the results are shown in Figure 2, where the blue color denotes the OAs, and the magenta color denotes the Kappa values. The solid lines denote the RoF method, while the dot dash lines represent the SSRoF method. The figure indicates that when the number of features involved in each subset increases, i.e., the number of feature subsets (K) decreases, the classification results tend to degenerate for both RoF and SSRoF. In fact, this is also consistent with the conclusions of [32], and that is why we selected a small number of M for the RoRF-KPCA method. Although when the training set increased, this problem seemed to be alleviated in a manner (for instance, in Figure 2e, 91.48% for $M = 5$ and 90.94% for $M = 30$ (SSRoF), when 20% of training samples were used), a small value of M is usually preferred. However, on the other hand, a smaller M means a larger K , which means the rotation process will be executed more times, and this will lead to a huge computational cost. Apart from the above analysis, we can also see that the proposed approach seemed to be more stable than RoF with the increment in the number of features per subset.

**Figure 2.** Cont.

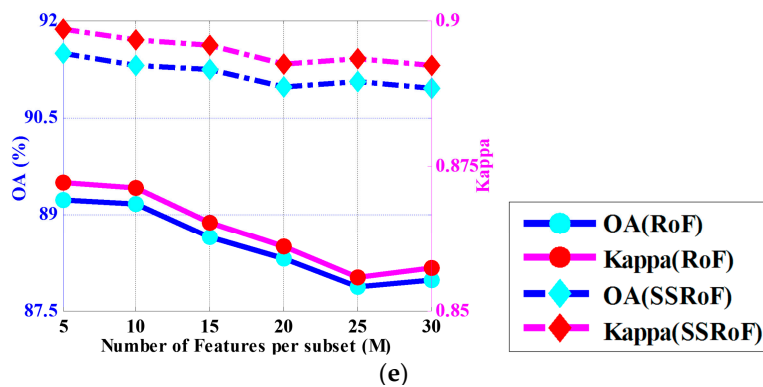


Figure 2. Impact of the number of features in each subset (M) under different numbers of training samples (1%, 2%, 5%, 10%, and 20% from (a–e), respectively).

4. Conclusions

Since existing rotation forest-based techniques fail to take account of the discriminative information of training samples during feature extraction, this paper proposed a semi-supervised rotation forest that uses the weighted semi-supervised local discriminant analysis method to jointly utilize the class discriminative information and local structural information provided by the labeled and unlabeled samples, respectively. The proposed algorithm aims to find the projection directions that provide better class separability, thus enhancing the performance of existing rotation forest algorithms. Furthermore, the proposed algorithm does not need additional parameters compared with the classical rotation forest method, which makes it easy to implement. Experiments have shown that the proposed algorithm outperforms several typical ensemble learning methods. Our future work will aim to reduce the computational time and assemble some other state-of-the-art machine learning algorithms.

Acknowledgments: This work was supported by the National Natural Science Foundation of China under Grant 61271348 and 61471148, and in part by the Foundation of Harbin Excellent Scholar under Grant 2015RAXXJ048. The authors would like to thank D. Landgrebe of Purdue University, West Lafayette, Indiana, for providing the AVIRIS Indian Pines data set; P. Gamba of the University of Pavia, Italy, for providing the Pavia University data sets; and the Hyperspectral Image Analysis group and the NSF-NCALM at the University of Houston for providing the Houston University data set.

Author Contributions: Xiaochen Lu and Junping Zhang conceived and designed the experiments; Xiaochen Lu and Tong Li performed the experiments; all authors analyzed the data and reviewed the study; Xiaochen Lu wrote the paper.

Conflicts of Interest: The authors declare no conflict of interest.

References

- Ballanti, L.; Blesius, L.; Hines, E.; Kruse, B. Tree species classification using hyperspectral imagery: A comparison of two classifiers. *Remote Sens.* **2016**, *8*, 445. [CrossRef]
- Sami ul Haq, Q.; Tao, L.; Yang, S. Neural network based Adaboosting approach for hyperspectral data classification. In Proceedings of the 2011 International Conference on Computer Science and Network Technology (ICCSNT), Harbin, China, 24–26 December 2011.
- Melgani, F.; Bruzzone, L. Classification of hyperspectral remote sensing images with support vector machines. *IEEE Trans. Geosci. Remote Sens.* **2004**, *42*, 1778–1790. [CrossRef]
- Li, J.; Bioucas-Dias, J.; Plaza, A. Semisupervised hyperspectral image segmentation using multinomial logistic regression with active learning. *IEEE Trans. Geosci. Remote Sens.* **2010**, *11*, 4085–4098. [CrossRef]
- Persello, C.; Bruzzone, L. Active and semisupervised learning for the classification of remote sensing images. *IEEE Trans. Geosci. Remote Sens.* **2014**, *52*, 6937–6956. [CrossRef]
- Villa, A.; Chanussot, J.; Benediktsson, J.A.; Jutten, C. Spectral unmixing for the classification of hyperspectral images at a finer spatial resolution. *IEEE J. Sel. Top. Signal Process.* **2011**, *5*, 521–533. [CrossRef]

7. Golipour, M.; Ghassemian, H.; Mirzapour, F. Integrating hierarchical segmentation maps with MRF prior for classification of hyperspectral images in a Bayesian framework. *IEEE Trans. Geosci. Remote Sens.* **2016**, *54*, 805–816. [[CrossRef](#)]
8. Licciardi, G.; Pacifici, F.; Tuia, D.; Prasad, S.; West, T.; Giacco, F.; Thiel, C.; Inglada, J.; Christophe, E.; Chanussot, J.; et al. Decision fusion for the classification of hyperspectral data: Outcome of the 2008 GRSS data fusion contest. *IEEE Trans. Geosci. Remote Sens.* **2009**, *47*, 3857–3865. [[CrossRef](#)]
9. Wozniak, M.; Graña, M.; Corchado, E. A survey of multiple classifier systems as hybrid systems. *Inf. Fusion* **2014**, *16*, 3–17. [[CrossRef](#)]
10. Krawczyk, B.; Minku, L.L.; Gama, J.; Stefanowski, J.; Wozniak, M. Ensemble learning for data stream analysis: A survey. *Inf. Fusion* **2017**, *37*, 132–156. [[CrossRef](#)]
11. Santos, A.B.; Araújo, A.A.; Menotti, D. Combining multiple classification methods for hyperspectral data interpretation. *IEEE J. Sel. Top. Appl. Earth Obs. Remote Sens.* **2013**, *6*, 1450–1459. [[CrossRef](#)]
12. Waske, B.; Linden, S.V.D.; Benediktsson, J.A.; Rabe, A.; Hostert, P. Sensitivity of support vector machines to random feature selection in classification of hyperspectral data. *IEEE Trans. Geosci. Remote Sens.* **2010**, *2880*–2889. [[CrossRef](#)]
13. Wang, S.; Yao, X. Relationships between diversity of classification ensembles and single-class performance measures. *IEEE Trans. Knowl. Data Eng.* **2013**, *25*, 206–219. [[CrossRef](#)]
14. Galar, M.; Fernandez, A.; Barrenechea, E.; Bustince, H.; Herrera, F. A review on ensembles for the class imbalance problem: Bagging-, Boosting-, and hybrid-based approaches. *IEEE Trans. Syst. Man Cybern.—Part C: Appl. Rev.* **2012**, *42*, 463–484. [[CrossRef](#)]
15. Friedman, J.H. Greedy function approximation: A gradient boosting machine. *Ann. Stat.* **2001**, *29*, 1189–1232. [[CrossRef](#)]
16. Breiman, L. Bagging predictors. *Mach. Learn.* **1996**, *24*, 123–140. [[CrossRef](#)]
17. Schapire, R.E. The strength of weak learn ability. *Mach. Learn.* **1990**, *5*, 197–227. [[CrossRef](#)]
18. Schapire, R.E.; Singer, Y. Improved boosting algorithms using confidence-rated predictions. *Mach. Learn.* **1999**, *37*. [[CrossRef](#)]
19. Ho, T.K. The random subspace method for constructing decision forests. *IEEE Trans. Pattern. Anal. Mach. Intell.* **1998**, *20*, 832–844. [[CrossRef](#)]
20. Breiman, L. Random forests. *Mach. Learn.* **2001**, *45*, 5–32. [[CrossRef](#)]
21. Ham, J.; Chen, Y.; Crawford, M.M.; Ghosh, J. Investigation of the random forest framework for classification of hyperspectral data. *IEEE Trans. Geosci. Remote Sens.* **2005**, *43*, 492–501. [[CrossRef](#)]
22. Xia, J.; Liao, W.; Chanussot, J.; Du, P.; Song, G.; Philips, W. Improving random forest with ensemble of features and semisupervised feature extraction. *IEEE Geosci. Remote Sens. Lett.* **2015**, *12*, 1471–1475. [[CrossRef](#)]
23. Chan, J.C.; Paelinckx, D. Evaluation of random forest and Adaboost tree-based ensemble classification and spectral band selection for ecotope mapping using airborne hyperspectral imagery. *Remote Sens. Environ.* **2008**, *112*, 2999–3011. [[CrossRef](#)]
24. Rodriguez-Galianoa, V.F.; Ghimireb, B.; Roganb, J.; Chica-Olmoa, M.; Rigol-Sanchezc, J.P. An assessment of the effectiveness of a random forest classifier for land-cover classification. *ISPRS J. Photogramm. Remote Sens.* **2012**, *67*, 93–104. [[CrossRef](#)]
25. Merentitis, A.; Debes, C.; Heremans, R. Ensemble learning in hyperspectral image classification: Toward selecting a favorable bias-variance tradeoff. *IEEE J. Sel. Top. Appl. Earth Obs. Remote Sens.* **2014**, *7*, 1089–1102. [[CrossRef](#)]
26. Gurram, P.; Kwon, H. Sparse kernel-based ensemble learning with fully optimized kernel parameters for hyperspectral classification problems. *IEEE Trans. Geosci. Remote Sens.* **2013**, *51*, 787–802. [[CrossRef](#)]
27. Samat, A.; Du, P.; Liu, S.; Li, J.; Cheng, L. E2LMs: Ensemble extreme learning machines for hyperspectral image classification. *IEEE J. Sel. Top. Appl. Earth Obs. Remote Sens.* **2014**, *7*, 1060–1069. [[CrossRef](#)]
28. Guo, H.; Li, Y.; Jennifer, S.; Gu, M.; Huang, Y.; Gong, B. Learning from class-imbalanced data: Review of methods and applications. *Expert Syst. Appl.* **2017**, *73*, 220–239. [[CrossRef](#)]
29. Merentitis, A.; Debes, C. Many hands make light work—on ensemble learning techniques for data fusion in remote sensing. *IEEE Geosci. Remote Sens. Mag.* **2015**, *3*, 86–99. [[CrossRef](#)]
30. Rodriguez, J.J.; Kuncheva, L.I. Rotation forest: A new classifier ensemble method. *IEEE Trans. Pattern Anal. Mach. Intell.* **2006**, *28*, 1619–1630. [[CrossRef](#)] [[PubMed](#)]

31. Ayerdi, B.; Romay, M.G. Hyperspectral image analysis by spectral-spatial processing and anticipative hybrid extreme rotation forest classification. *IEEE Trans. Geosci. Remote Sens.* **2016**, *54*, 2627–2639. [[CrossRef](#)]
32. Xia, J.; Falco, N.; Benediktsson, J.A.; Du, P.; Chanussot, J. Hyperspectral image classification with rotation random forest via KPCA. *IEEE J. Sel. Top. Appl. Earth Obs. Remote Sens.* **2017**, *10*, 1601–1609. [[CrossRef](#)]
33. Chen, J.; Xia, J.; Du, P.; Chanussot, J. Combining rotation forest and multiscale segmentation for the classification of hyperspectral data. *IEEE J. Sel. Top. Appl. Earth Obs. Remote Sens.* **2016**, *9*, 4060–4072. [[CrossRef](#)]
34. Rahulamathavan, Y.; Phan, R.C.-W.; Chambers, J.A.; Parish, J.D. Facial expression recognition in the encrypted domain based on local Fisher discriminant analysis. *IEEE Trans. Affect. Comput.* **2013**, *4*, 83–92. [[CrossRef](#)]
35. Belhumeur, P.N.; Hespanha, J.P.; Kriegman, D.J. Eigenfaces vs. Fisherfaces: Recognition using class specific linear projection. *IEEE Trans. Pattern Anal. Mach. Intell.* **1997**, *19*, 711–720. [[CrossRef](#)]
36. Lu, X.; Zhang, J.; Li, T.; Zhang, G. Synergetic classification of long-wave infrared hyperspectral and visible images. *IEEE J. Sel. Top. Appl. Earth Obs. Remote Sens.* **2015**, *8*, 3546–3557. [[CrossRef](#)]
37. Sun, B.; Kang, X.; Li, S.; Benediktsson, J.A. Random-walker-based collaborative learning for hyperspectral image classification. *IEEE Trans. Geosci. Remote Sens.* **2017**, *55*, 212–222. [[CrossRef](#)]
38. Kang, X.; Li, S.; Benediktsson, J.A. Feature extraction of hyperspectral images with image fusion and recursive filtering. *IEEE Trans. Geosci. Remote Sens.* **2014**, *52*, 3742–3752. [[CrossRef](#)]
39. Kang, X.; Zhang, X.; Li, S.; Li, K.; Li, J.; Benediktsson, J.A. Hyperspectral anomaly detection with attribute and edge-preserving filters. *IEEE Trans. Geosci. Remote Sens.* **2017**, 1–12. [[CrossRef](#)]
40. Sugiyama, M.; Idé, T.; Nakajima, S.; Sese, J. Semi-supervised local Fisher discriminant analysis for dimensionality reduction. *Mach. Learn.* **2010**, *78*, 35–61. [[CrossRef](#)]
41. Sugiyama, M. Dimensionality reduction of multimodal labeled data by local Fisher discriminant Analysis. *J. Mach. Learn. Res.* **2007**, *8*, 1027–1061. [[CrossRef](#)]
42. He, X.; Niyogi, P. Locality preserving projections. In *Advances in Neural Information Processing Systems*; MIT Press: Cambridge, MA, USA, 2004; pp. 153–160.
43. Martinez, M.; Kak, A.C. PCA versus LDA. *IEEE Trans. Pattern Anal. Mach. Intell.* **2001**, *23*, 228–233. [[CrossRef](#)]
44. He, X.; Cai, D.; Yan, S.; Zhang, H. Neighborhood preserving embedding. In Proceedings of the Tenth IEEE International Conference on Computer Vision, Beijing, China, 17–20 October 2005; pp. 1208–1213.
45. Liao, W.; Pi, Y. Feature extraction for hyperspectral images based on semi-supervised local discriminant analysis. In Proceedings of the 2011 Joint Urban Remote Sensing Event (JURSE), Munich, Germany, 11–13 April 2011; pp. 401–404.
46. Bao, R.; Xia, J.; Mura, M.D.; Du, P.; Chanussot, J.; Ren, J. Combining morphological attribute profiles via an ensemble method for hyperspectral image classification. *IEEE Geosci. Remote Sens. Lett.* **2016**, *13*, 359–363. [[CrossRef](#)]
47. Xia, J.; Mura, M.D.; Chanussot, J.; Du, P.; He, X. Random subspace ensembles for hyperspectral image classification with extended morphological attribute profiles. *IEEE Trans. Geosci. Remote Sens.* **2015**, *53*, 4768–4785. [[CrossRef](#)]
48. Xia, J.; Du, P.; He, X.; Chanussot, J. Hyperspectral remote sensing image classification based on rotation forest. *IEEE Geosci. Remote Sens. Lett.* **2014**, *11*, 239–243. [[CrossRef](#)]

